SCExAO: lessons learned for a future TMT instrument

Julien Lozi[a], Olivier Guyon[a,b,c,d], Nemanja Jovanovic[a,e,f], Sean Goebel[a,g], Prashant Pathak[a,h], Barnaby Norris[i], Frantz Martinache[j], Mamadou N'Diaye[j], Ben Mazin[k], and Alex Walter[k]

[a]National Astronomical Observatory of Japan, Subaru Telescope, National Institutes of Natural Sciences (NINS), 650 North A'ohōkū Place, Hilo, HI 96720, U.S.A.
[b]Steward Observatory, University of Arizona, Tucson, AZ 85721, U.S.A.
[c]College of Optical Sciences, University of Arizona, Tucson, AZ 85721, U.S.A.
[d]Astrobiology Center of NINS, 2-21-1, Osawa, Mitaka, Tokyo, 181-8588, Japan
[e]Department of Physics and Astronomy, Macquarie University, NSW 2109, Australia
[f]California Institute of Technology, 1200 E California Blvd, Pasadena, CA 91125, U.S.A.
[g]Institute for Astronomy, University of Hawai'i, 640 North A'ohōkū Place, Hilo, HI 96720, U.S.A.
[h]Sokendai University, 1560-35 Kamiyamaguchi, Hayama, 240-0115, Japan
[i]University of Sidney, NSW 2006, Australia
[j]Observatoire de la Côte d'Azur, Boulevard de l'Observatoire, Nice, 06304, France
[k]University of California Santa Barbara, Santa Barbara, CA 93106, U.S.A

ABSTRACT

The Subaru Coronagraphic Extreme Adaptive Optics (SCExAO) instrument has evolved tremendously for the past few years. Its modular design is an asset to test new technologies and functionalities. Although ExAO capabilities were only achieved recently, providing high-contrast images of a new disk and several known targets, lessons have already been learned for future ELT instruments. Some critical issues were identified during the development, forcing us to rethink the priorities of the wavefront correction.

Telescope vibrations were carefully characterized, using accelerometers and wavefront sensors (WFS) telemetry. This analysis shaped a new vibration mitigation scheme, using the accelerometer data and more advanced predictive control. The low-wind effect (LWE) that splits the PSF was also measured. Although the LWE is not naturally present on the telescope, it can be artificially created by pupil misalignments in the Pyramid WFS (PyWFS). The sensitivity of the PyWFS to the LWE modes was measured and showed that a trade-off has to be made between sensitivity and accuracy. We are currently developing and testing focal plane WFS approaches to address this effect.

Performing the ExAO correction independently behind a pre-existing classical AO system has the great advantage of simplifying the design and development of the instrument, but it has some practical limits. Communication is necessary between the various control loops. We are now converging on a design with better communication, better hardware, and multiple WFS in visible and infrared, to be more adaptable to the targets we observe. These lessons will be invaluable for designing an optimized high-contrast imager for TMT and other ELTs.

Keywords: extreme adaptive optics, exoplanets, wavefront control, GPU, low latency, pyramid wavefront sensor, focal plane wavefront sensor, low-order wavefront sensor

Further author information: (Send correspondence to J.L.)
J.L.: E-mail: lozi@naoj.org, Telephone: 1 808 934 5949

1. INTRODUCTION

The high-contrast observation of exoplanets requires more and more complex wavefront sensors, to correct every aspects of wavefront errors degrading the quality of the image. The Subaru Coronagraphic Extreme Adaptive Optics (SCExAO) instrument, the high contrast instrument installed on the Subaru telescope, combines multiple wavefront sensing techniques, to achieve the best possible contrast at small inner working angles. SCExAO is installed behind AO188, the facility adaptive optics of Subaru. AO188 performs a first stage of correction of the atmospheric turbulence, delivering Strehl ratios between 30 and 40% in H-band. A Pyramid Wavefront Sensor (PyWFS) performs a second stage of correction, removing most of the residual wavefront errors. Then an Asymmetric Pupil Fourier Wavefront Sensor (APF-WFS), also called the Zernike Asymmetric Pupil (ZAP) wavefront sensor, remove quasi-static low-order aberration at the beginning of an observation. If a low inner working angle coronagraph is used, a coronagraphic Lyot-stop Low-Order Wavefront Sensor (LLOWFS) takes care of the chromatic residual low-order aberrations occurring upstream of the coronagraphic focal plane mask. Finally, a focal plane wavefront sensor like speckle nulling can be added to improve the detection limit on one half of the focal plane, by removing residual slow-varying speckles.

SCExAO is testing several critical technologies for future first generation high-contrast imagers on Giant Segmented Mirror Telescopes (GSMTs) like the Thirty Meter Telescope (TMT), partly funded by Japan. The lessons learned on SCExAO will be crucial in the design of these instruments, to reach the goal of imaging Earth-like planets around M-type stars.

The current architecture of SCExAO, despite its modular advantage, presents a lot of challenges for wavefront control. Indeed, the first stage of correction provided by AO188 provides a cleaned-up wavefront at the entrance of SCExAO, putting less constraints on the stroke of its DM, and keeping all the optics relatively small. But the current lack of communication between AO188 and SCExAO showed some limitations, that can be address in the near future with some hardware and software upgrades, as explained in Sec. 2.

Another challenge comes from the fact that a single DM has to combine the correction of several wavefront sensors (WFS). The multiple measurements have to be combined optimally to send a single command to the DM and avoid any conflict between the loops. Section 3 explains how the wavefront control loops are connected to each other, and how the use fo a coronagraph can dramatically improve on-sky use of algorithms like speckle nulling.

Finally, Sec. 4 explores how SCExAO is dealing with the known issue of telescope vibrations and the newly found issue of low-wind effect (also known as island effect). These two type of disturbance can degrade dramatically the wavefront correction and the detectability of faint sources. New technologies like the SAPHIRA detector and the Microwave Kinetic Inductance Detector (MKID) will help tackle these issues and allow for a better control of the speckle field.

2. WAVEFRONT CONTROL ARCHITECTURE OF SCExAO

2.1 Current Wavefront Control Architecture and Limitations

SCExAO is a unique instrument dedicated for testing new technologies for future ELTs, as well as doing compelling science on a 8-m telescope. Following that vision, SCExAO was developed using the first stage of correction provided by Subaru's facility adaptive optics AO188. AO188 uses a curvature wavefront sensor with Avalanch Photodiodes (APDs) and a 188-actuator bi-morph deformable mirror (DM) to achieve H-band Strehl ratios up to 30-40%.[1] During SCExAO observations, AO188 uses the light bellow 600 nm to perform its wavefront correction. The rest of the light is sent to the SCExAO instrument, where it is distributed to the various wavefront sensors and module. For a full description of the various modules of SCExAO, see[2] and Nem Jovanovic's paper in these proceedings.

Figure 1 presents the wavefront control architecture of SCExAO, with the various loops correcting different aspects of the wavefront residuals. The light is first reflected by SCExAO's 2000-actuator DM. The light is then split between visible (600-950 nm) and NIR (950-2500 nm). Most of the residual wavefront errors left by AO188 are then measured and corrected by the extreme-AO loop, which uses a pyramid optics (see Sec. 4.1, an First Light Imaging OCAM2K EMCCD camera and the 2k-actuator DM. This loop corrects about 1200 modes

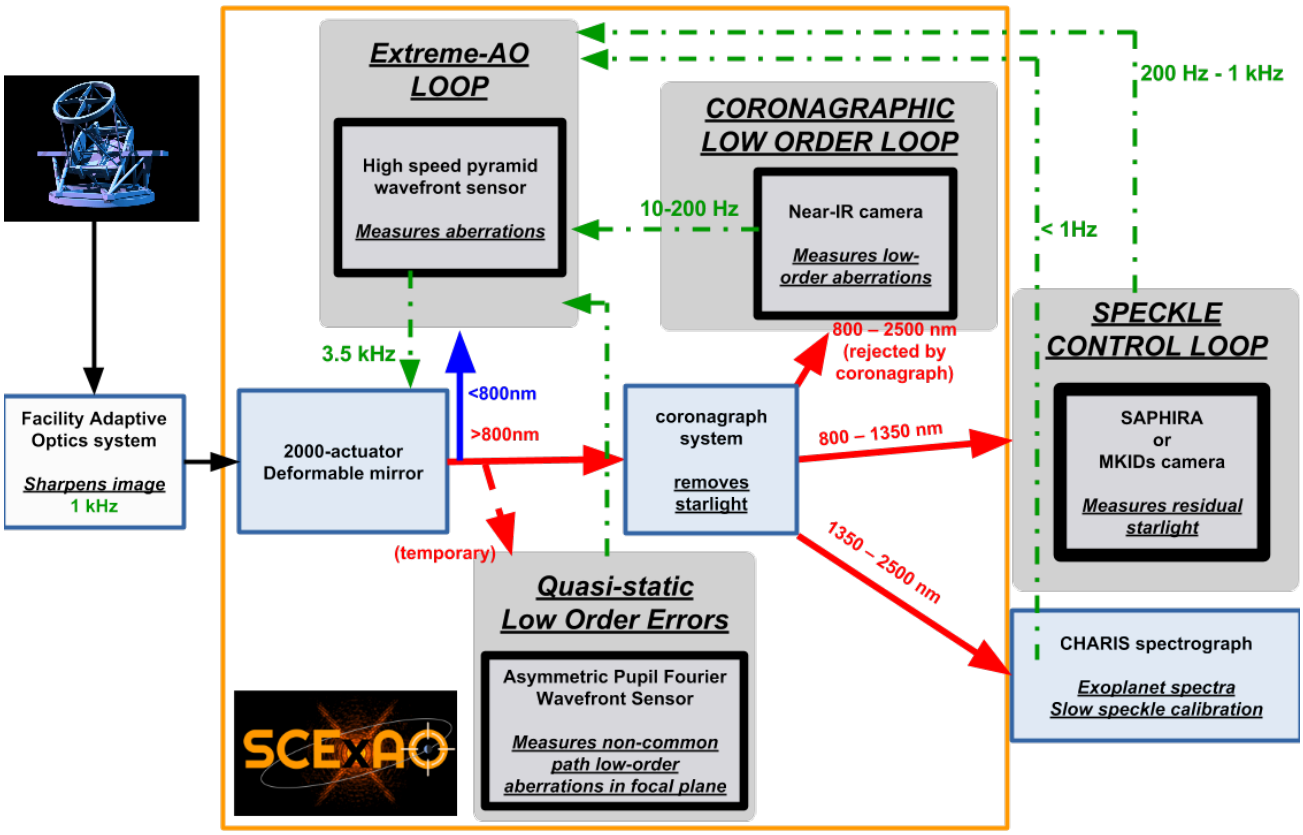

Figure 1. Wavefront control architecture of SCExAO.

of dynamical aberrations at up to 3.5 kHz. We currently achieve 90% Strehl ratio in good seeing conditions (<0.5").

Each secondary control loop has it's own purpose, and rely on the correction of the ExAO loop to perform optimally. The quasi-static low-order errors —non-common path errors unseen by the PyWFS— are measured and corrected by the ZAP WFS[3] (see Sec. 4.3). dynamic low-order errors, due mainly to the chromaticity of the atmosphere, are measured inside the coronagraph, by the coronagraphic LLOWFS[4] (See Sec. 4.3). Finally, static and dynamic high-order aberrations are corrected with the speckle control loop —depending on the speed of the camera used (see Sec. 3.2.

The main limitation in the current wavefront control architecture presented in Fig. 1 is that there is no communication between AO188 and SCExAO. Since the hardware and software of AO188 is relatively old, it is not easy to implement any kind of communication to transfer some telemetry, or send commands to its DM. This issue is limiting us to achieve the goal of an optimal correction of the wavefront. But as we will see in the next section, upgrades are being made that will allow greater communication between the two systems.

2.2 Future Upgrades to AO188

A few upgrades are planed for AO188 upstream of SCExAO, that will allow a better communication between the two instruments, and better overall performances.

2.2.1 Real-time computer upgrades

A new computer was recently purchased to replace the old real-time computer (RTC) of AO188. It is currently in a phase of tests, to make it compatible with the old hardware (APDs and DM driver mostly). The software architecture will reuse what have been developed for SCExAO, especially with the use of GPUs for fast real-time computations. This new computer will also allow to analyze and save real-time telemetry from the system, a

functionality that is currently lacking in AO188. This will help in the debugging of SCExAO's performances in various conditions.

This new RTC will also allow more communications between the instruments: AO188's telemetry will be used by SCExAO to adjust its loop parameters, and SCExAO can even control directly AO188's DM. In the long term, we will be able to have AO188 and SCExAO in a woofer-tweeter configuration, allowing for more optimized wavefront correction.

2.2.2 Hardware upgrades

A beam switcher is currently under development in collaboration with the Australian National University (ANU). This component will be installed behind AO188 to perform an easy switch between SCExAO and the Infrared Camera and Spectrograph (IRCS), and even allow them to work at the same time, with the use of dichroics.

We also plan to include an Infrared PyWFS (see Sec. 4.1) on SCExAO, using a FirstLight Imaging C-RED1 or potentially the SPAHIRA camera developed by the Institute for Astronomy (IfA)[5] (see paper by Sean Goebel in this proceedings). Thanks to the beam switcher, the correction from this PyWFS could be used by IRCS or any other infrared instrument.

AO188's old hardware will also be replaced with more efficient technologies. The curvature wavefront sensor using APDs will be upgraded with a PyWFS, similar to the one inside SCExAO, using a First Light Imaging OCAM2K as the detector. The 188-actuator bimoprh DM will be replaced with a 64x64-actuator DM, that will give AO188 ExAO capabilities even without SCExAO. In that configuration, SCExAO's 2000-actuator DM would be exclusively used for speckle control to achieve higher contrast in one half of the image (see Sec. 3.2).

These upgrades will make the combination AO188+SCExAO the ultimate testbed for a first generation high-contrast imager for TMT and other GSMTs.

3. WAVEFRONT CONTROL WITH ONE DEFORMABLE MIRROR

3.1 Using One Deformable Mirror with Multiple Wavefront Sensors

As we saw in Sec. 2.1, SCExAO is equipped with a unique 2000-actuator DM, and multiple wavefront sensors. Since the various wavefront control loops cannot send independent commands to DM without conflict, Only one loop sends the commands: the ExAO loop. As explained in the schematics in Fig. 2, the other wavefront control loops send their commands to the PyWFS loop, in the form of an offset to the PyWFS loop reference, as well as a DM command. The DM commands coming from the various sources are then co-added into a single DM map that is sent to the DM, while the reference of the PyWFS loop is also simultaneously updated using the offsets. That way, the changes coming from the other loops are not affecting the PyWFS correction, and the PyWFS does not try to compensate for the other corrections.

This method works well for small amplitude corrections. But if the amplitude is too high, the PyWFS can end up in a non-linear regime and become unstable. That is why it is necessary to keep the maximum amplitude of the commands coming from the various loop to a small value, typically about 100 to 200 nm. This value depends a lot on the modulation radius of the PyWFS, and the starting point of the loop.

3.2 Creating a Dark Hole On-Sky with Speckle Nulling

To improve the contrast in the image, speckles have to be removed in some way. One method to deal with this issue is to use the DM to create "anti-speckles" that will interfere destructively with the speckles already present in the image. The easiest method to do that is called speckle nulling. The brightest speckles are identified in the image, for which amplitudes and positions are measured. With these informations, speckles are created using sinewaves on the DM, at the exact same spatial frequencies, and with similar amplitudes. The phases of the sinewaves are then scanned using about 10 positions. For each speckle, the optimal set of parameters is then applied. A few tens of speckles are corrected at the same time, and the control is performed in an iterative loop, until the maximum contrast is reached. This method only allow the correction on one half of the speckle field, when only one DM is used.

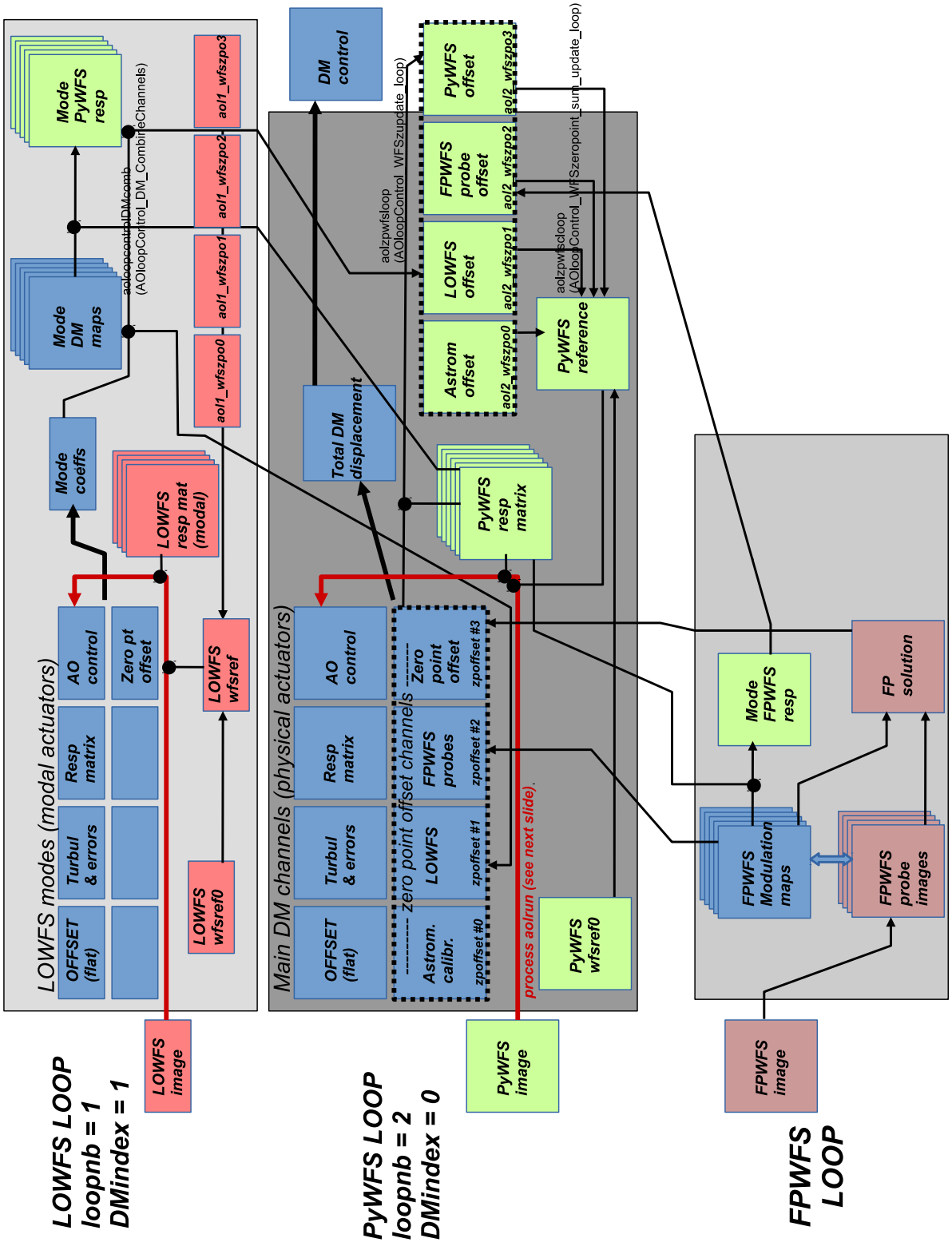

Figure 2. Schematic presenting the interactions between the various loops. Blue square are commands in DM space, while green square are images in WFS space. The main loop uses the the PyWFS and sends commands to the DM. The other loops send offsets simultaneously in DM space and WFS space to perform a correction using the DM.

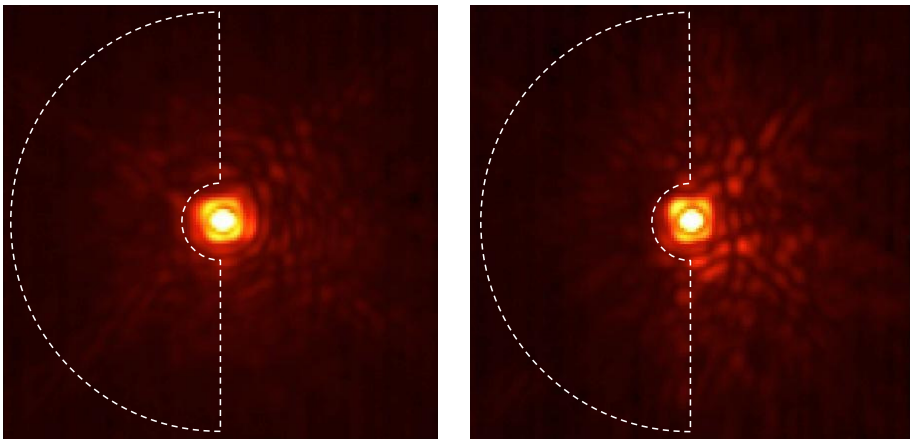

Figure 3. On-sky correction of speckles on one side of the science plane using speckle nulling (white region): before correction (left) and after correction (ight).

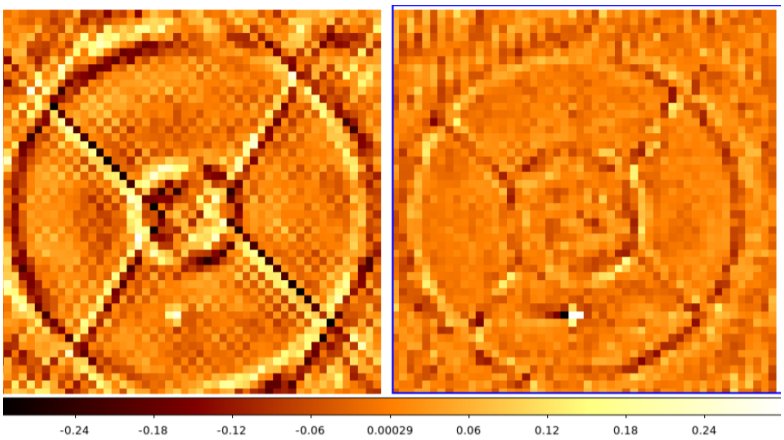

Figure 4. Correction maps applied on the DM for speckle nulling without coronagraph (left) and with a simple Lyot coronagraph (right). The edges of the Subaru pupil can be seen on the left, while the edges of the Lyot stop can be seen on the right. The amplitude of the corrections on the DM is more than 3 times smaller when the coronagraph is used.

It is possible to calculate a correction map using the internal calibration source, and use that same map in a static way on-sky. That is what have been tested so far when combined with the PyWFS. Figure 3 present such a result on the star RX Boo.[6] In this example, the PyWFS was not used, the wavefront correction was only coming from AO188. Also no coronagraph was used, so the speckle nulling was mostly correcting quasi-static speckles created by the diffraction of the pupil.

The problem with not using a coronagraph is that the amplitude needed on the DM to compensate for diffraction speckles is quite high, especially at the edge of the pupil. Most of these speckles can be controlled by adding a coronagraph in the beam. Any type of coronagraph remove the light from the core of the star, but also takes care of most of the speckles around the star, especially the ones created by the diffraction of the edges of the pupil, and by the spiders. If speckle nulling is performed after a coronagraph, the amplitude used on the DM to correct for the speckles is much less, and more friendly to the PyWFS. Figure 4 presents a comparison of the control maps calculated with the speckle nulling, when there is no coronagraph (left) and when a simple Lyot coronagraph is present (right). With a coronagraph, the amplitudes of the corrections performed by the DM are about 3 times smaller than without a coronagraph. On-sky, the PyWFS struggles to keep its stability when the left map is applied: the high amplitude creates some non-linear effect inside the PyWFS, especially at the edge of the pupil. But with a coronagraph, the map is much more adapted to the linear range of the PyWFS, and can be applied with no trouble.

The next step is to use this kind of map as a starting point to a dynamic correction using a fast IR camera, like

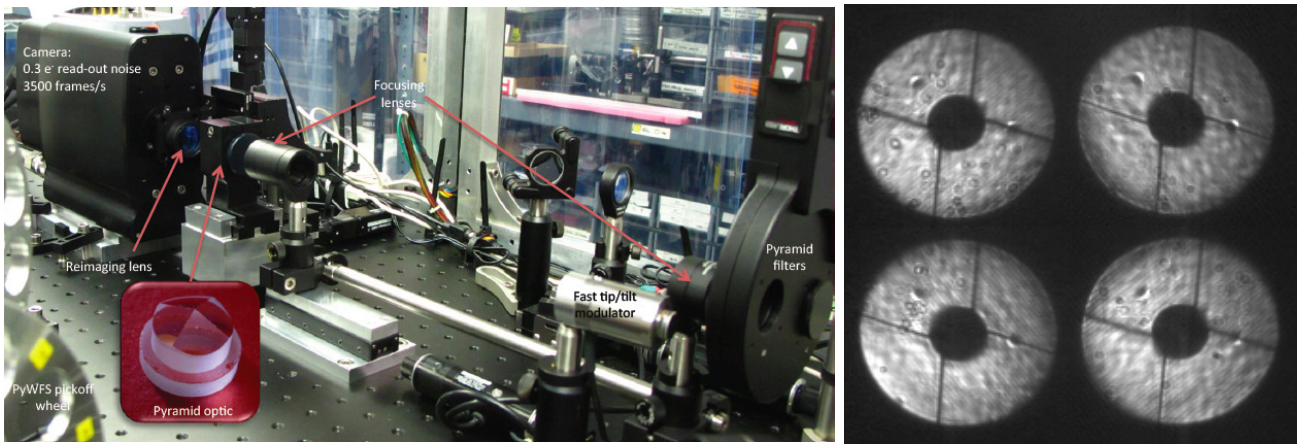

Figure 5. PyWFS hardware in the SCExAO instrument (left) and PyWFS pupil image taken with the camera OCAM2k (right).

the SAPHIRA camera from IfA,[5] or the MKIDs detector from University of California Santa Barbara (UCSB).[7] These new generations of detector will allow for a fast control in photon counting regime of the dynamic speckles.

4. NEW WAVEFRONT SENSING TECHNIQUES AND HARDWARE FOR OLD AND NEW PROBLEMS

4.1 Visible and Infrared Pyramid Wavefront Sensor

The main wavefront sensor of SCExAO is the Pyramid Wavefront Sensor (PyWFS). The sensor uses part of the visible light, usually from 800 nm to 900 nm, although it can be extended at shorter wavelengths to 700 nm, for fainter targets. As seen in Fig. 5 (left), the camera used is the OCAM^{2}k from First Light Imaging, a 240×240-pixel EMCCD, with a frame rate of 2 kHz. In binned mode (120×120 pixels), the camera can run up to 3.6 kHz.

Before reaching the camera, the beam goes through several optics. The pupil is imaged on a fast steering mirror (FSM), from Physik Instrumente. The FSM modulates the beam circularly using sinewave generators. The frequency of the modulation is also controlling the frame rate of the camera to have a full circle of modulation per frame. The radius of motion is about 3 λ/D, although it can be reduced to almost 0 depending on the turbulence level and the quality of correction. The setup is presented in Fig. 5 (left), while a lab image of the four pupils imaged by the OCAM2K camera is shown in Fig. 5 (right).

The PyWFS demonstrated a few limitations that need more development. The first one is the variation of the optical gain depending on the level of correction. This issue makes the PyWFS hard to calibrate absolutely, which is essential for algorithms like predictive control (see Sec. 4.2) or the calculation of optimal loop gain for each mode. The second main issue is the difficulty of the PyWFS to measure island or low-wind effect modes (see Noah Schwartz's paper in these proceedings). These modes that are defined by the four segments in the pupil separated by the thick spiders of Subaru, are usually not well measured and therefore corrected by the PyWFS. This sensitivity issue varies with spider thickness, modulation radius and current conditions (seeing and wind speed). As explained in Sec. 4.3, a dedicated focal plane WFS might be unavoidable to correct these modes.

New developments in hardware have also been tested in the last couple of years. The original pyramid optics, loaned by MagAO,[8] was replaced by a new design composed of two rooftop prisms 90 degrees from each other, presented in Fig. 6 (left). The edges of the two rooftop prisms are only a few tens of microns apart, and the intersection creates the apex of the pyramid where the beam is focused on. If the apex is somehow damaged, the prisms can just be translated to create a new clean apex.

A clone of this pyramid was also tested in front of the SAPHIRA detector to create the first demonstration of a NIR PyWFS. Since the SAPHIRA camera was not working at the current full speed, this NIR PyWFS was only tested on the laboratory source, by introducing about 300 nm RMS of Kolmogorov turbulence on the

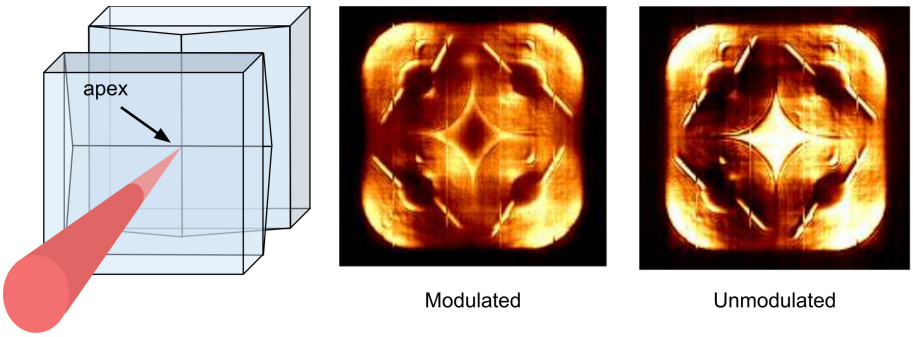

Figure 6. New concept of Pyramid optics using roof prisms (left), and demonstration of NIR PyWFS in modulated (center) and unmodulated modes (right).

DM at low speed. The loop was closed with and without modulation (see Fig. 6 center and right respectively). This first demonstration show the potential of the SAPHIRA detector for wavefront sensing, as well as the new pyramid optics design, in both modulated and unmodulated conditions.

4.2 Measuring and Correcting Telescope Vibrations

Telescope vibrations is a serious limitation for most high-contrast instruments. They are usually stronger than the atmospheric tip-tilt errors, and require a WFS with enough linear range and speed to be measured, and a DM with enough stroke to be corrected. In the case of the Subaru Telescope, vibrations can be as high as 0.5 arcsec rms, and are usually stronger when the target is transiting in the sky, i.e. at maximum elevation. To measure these vibrations, accelerometers where installed on the top ring of the telescope, holding the secondary mirror. Vibrations where measured during several SCExAO observing nights, on various targets. Comparing these measurements to WFS tip/tilt measurements, we found a strong correlation in the frequency and amplitude of the vibrations.[9] We also found out that the frequencies of the vibrations are usually linked to the speed of rotation of the telescope, both in azimuth and elevation. Finally, some strong vibrations are only visible around the transit of the target, and are due to an instability in the pointing control loop of the telescope in the elevation axis, when the telescope is almost static.

To correct for these vibrations, two methods of predictive control were tested. The first method is similar to the one used in SPHERE.[10] A model of the atmospheric turbulence and the vibrations is built using pseudo-open loop data reconstructed from real-time telemetry.[11] This model, updated every 30 second or so, is fed to a Linear Quadratic Gaussian (LQG) controller.[12] Figure 7 presents a example of correction using the LQG, by comparing the Power Spectrum Density (PSD) in closed-loop and in reconstructed pseudo-open loop, in two different conditions: when telescope vibrations are low (Fig. 7 (left)) and around transit when a strong vibration is present (Fig. 7 (right)). The figure shows a reduction of the atmospheric turbulence, as well as dips in the PSD where vibrations were identified. Even in the case of strong vibration, the resulting closed-loop PSD does not show any residual at the vibration's frequency. For more details on the correction, see.[9]

The second method used to correct vibration is a more simple approach to predictive control than the LQG controller. A model of the disturbance including both turbulence and vibrations is extracted from a dataset of past telemetry data. This model is inverted and used to predict the next data point. This method allow any kind of telemetry data to be added for increase precision. The goal is to use the telemetry from the PyWFS as well as accelerometer data to compute an optimal correction. This method is called sensor fusion, and was adapted from algorithms used to perform weather forecast. It is more powerful than the LQG for the prediction of non-regular but recurring patterns. For more details and some simulation results, see.[13]

4.3 Measurement and correction of Low-Wind Effect/Island modes

laboratory and on-sky experiments show that the PyWFS is not very sensitive to island modes (sometimes called Low-Wind Effect (LWE) modes). These modes, defined by the segmented geometry of the pupil and the spiders of the telescope, create a discontinuity behind the spiders than can split the PSF is several (2 to 4) cores. A PyWFS using a small modulation is more sensitive to these modes, but lacks the linear range to measure strong

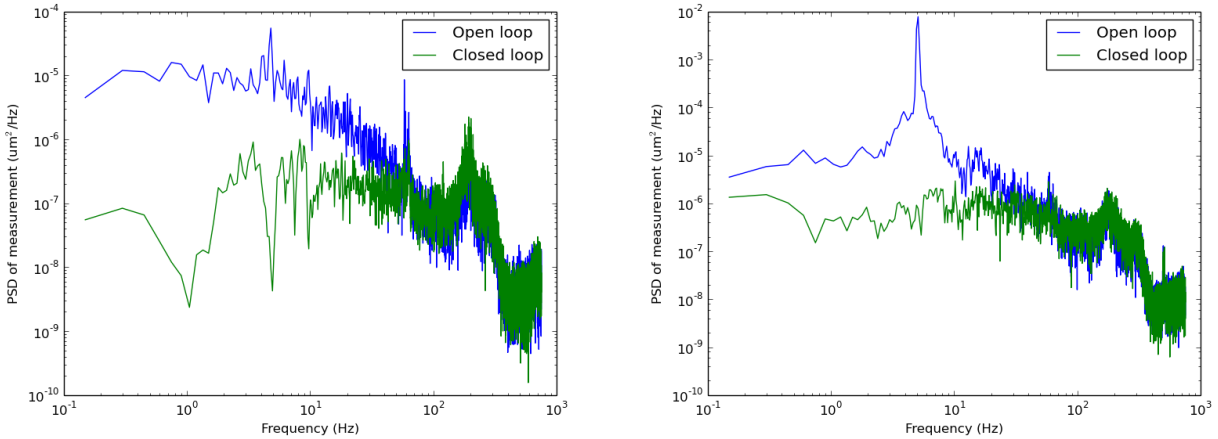

Figure 7. Demonstration of correction with the LQG controller: PSD of tip in pseudo-open loop and closed loop, in an average case (left) and during a strong transit vibration (right).

aberrations. A larger modulation makes the PyWFS more linear on a wider range, but reduces the sensitivity to the island modes. For a more detailed study of the measurement of island modes with the PyWFS, see Noah Schwartz's paper in these proceedings.

Since the island modes are much more obvious in the focal plane than the pupil plane, we tried to use the Zernike Asymmetric Pupil (ZAP) WFS[3] to measure them. An set of orthogonal modes was built and used for the calibration of the ZAP WFS. The linearity of the sensor was then measured for each modes. The results, presented in more details in Mamadou N'Diaye's paper in these proceedings, show that ZAP can indeed identify and close the loop on the island modes, but on a limited linear range of about 100 nm.

An other sensor could be used to measure the island modes: the coronagraphic Lyot stop Low-Order Wavefront Sensor (LLOWFS).[4] This versatile WFS uses the light rejected by the Lyot stop of the coronagraph to measure and correct low-order modes. It can measure a few tens of Zernike modes,[14] and can be used with any phase mask coronagraph.[15] Using island modes instead of Zernike modes (or an orthogonalized fusion of the two sets of modes), the LLOWFS could be able to measure and correct island modes. But like ZAP, it might be limited in linear range.

4.4 New detectors for wavefront sensing

SCExAO is an ideal platform to test new technologies, especially new types of detectors. As seen in Sec. 4.1, we are testing the SAPHIRA camera developed by IfA (see Sean Goebel's paper in these proceedings), a fast HgCdTe avalanche photodiode detector that can run up to a few kilohertz, and can be used either for speckle nulling or PyWFS. This type of Ir photon counting fast camera will be essential for high-contrast imagers on GSMTs, because they will allow to perform wavefront sensing (either in pupil or focal plane) closer to the wavelengths of interest, at the photon noise limit.

Another new type of detector will soon be tested on SCExAO: The Microwave Kinetic Inductance Detectors (MKIDs), with the MKIDs Exoplanet Camera (MEC, see Fig. 8 (left)). This detector, like SAPHIRA is a fast photon counting detector in infrared. But the particularity of MKIDs is the ability of measuring the energy of each photon, i.e. its wavelength, with a low resolution of about 10. The detector for MEC has 20,000 pixels (see Fig. 8 (right)), and will be used to perform an optimal speckle control. Indeed, the spectral information of the speckles will help in performing a better correction with the DM. The camera will be delivered in December, and should start on-sky test in January.

5. CONCLUSION AND PERSPECTIVE

The SCExAO instrument is a complex and modular instrument extremely useful for testing new technologies and algorithms necessary for the next generation of high-contrast instruments that will be installed on GSMTs like

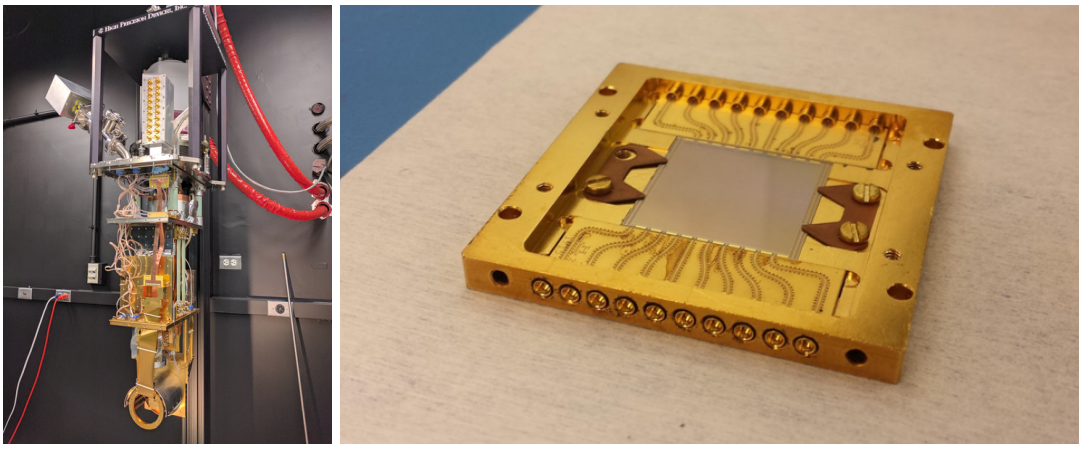

Figure 8. MKIDS Exoplanet Camera to be delivered at Subaru (left) and MKIDS 20k-pixel chip (right).

TMT. SCExAO demonstrated its capability to correct for atmospheric turbulence and other wavefront errors, during several engineering and science nights at the Subaru Telescope. But the current architecture of the instrument, despite being advantageous for its modularity, showed some limitations. The lack of communication between the first stage of correction provided by AO188 and the second stage inside of SCExAO is an issue that will be taken care of soon, with the upgrade of AO188's RTC. This new RTC will provide SCExAO with a better metrology, and SCExAO will be able to send commands to AO188's DM. In the long term, the combination of AO188 and SCExAO will be closer to a woofer/tweeter configuration. In the future, new hardware for AO188's wavefront sensor and DM will improve the performances, giving it ExAO capabilities.

Future instruments, like SCExAO, will combine several wavefront sensors, with only one or two DM to control. With SCExAO, we demonstrated that several WFS can indeed collaborate to send a unique command to the DM, by having secondary loops sending offsets to a primary loop, the ExAO loop. But this method has some limitations, especially in the amplitude of corrections that can be accepted by the primary loop. In the case of speckle nulling for example, a coronagraph is essential to remove most of the speckles created by diffraction, to reduce the constraints imposed on the DM. We demonstrated that a dark hole can be created on-sky, while the ExAO loop is running.

Two major issues faced by SCExAO will also impact future high-contrast instruments on GSMT: telescope vibrations and island modes. The first one was expected on this kind of instruments, but the difficulty to correct them was greater than expected. two methods of predictive control are being tested and show some promising results. The second issue, the island modes, were not anticipated before the first high-contrast instruments came on-line. This effect can have a dramatic impact on the PSF quality, and reduce significantly the detection of faint sources. A dedicated focal plane wavefront sensor, like ZAP or the LLOWFS, is probably the best solution to measure and correct these modes. New camera technologies like SAPHIRA or MKIDS will allow for a more precise wavefront correction in photon-counting mode in the near future.

SCExAO is building the path to the next generation of high-contrast instruments built for GSMTs. If all the upgrades suggested here are successful, SCExAO could even be the first high-contrast imager as a first light instrument on the Thirty Meter Telescope. The technologies tested here will be crucial to achieve the contrast necessary to image Earth-like planets around M-type stars.

ACKNOWLEDGMENTS

The authors acknowledge support from the JSPS (Grant-in-Aid for Research #23340051 & #26220704).

REFERENCES

[1] Minowa, Y., Hayano, Y., Oya, S., Watanabe, M., Hattori, M., Guyon, O., Egner, S., Saito, Y., Ito, M., Takami, H., Garrel, V., Colley, S., Golota, T., and Iye, M., "Performance of Subaru adaptive optics system AO188," in [*Adaptive Optics Systems II*], *Proc. Soc. Photo-Opt. Instrum. Eng.* **7736**, 77363N (July 2010).

[2] Jovanovic, N., Martinache, F., Guyon, O., Clergeon, C., Singh, G., Kudo, T., Garrel, V., Newman, K., Doughty, D., Lozi, J., Males, J., Minowa, Y., Hayano, Y., Takato, N., Morino, J., Kuhn, J., Serabyn, E., Norris, B., Tuthill, P., Schworer, G., Stewart, P., Close, L., Huby, E., Perrin, G., Lacour, S., Gauchet, L., Vievard, S., Murakami, N., Oshiyama, F., Baba, N., Matsuo, T., Nishikawa, J., Tamura, M., Lai, O., Marchis, F., Duchene, G., Kotani, T., and Woillez, J., "The Subaru Coronagraphic Extreme Adaptive Optics System: Enabling High-Contrast Imaging on Solar-System Scales," *Pub. Astron. Soc. Pacific* **127**, 890–910 (Oct. 2015).

[3] Martinache, F., Jovanovic, N., and Guyon, O., "Closed-loop focal plane wavefront control with the SCExAO instrument," *Astron. Astrophys.* **593**, A33 (Sept. 2016).

[4] Singh, G., Martinache, F., Baudoz, P., Guyon, O., Matsuo, T., Jovanovic, N., and Clergeon, C., "Lyot-based Low Order Wavefront Sensor for Phase-mask Coronagraphs: Principle, Simulations and Laboratory Experiments," *Pub. Astron. Soc. Pacific* **126**, 586–594 (June 2014).

[5] Atkinson, D., Hall, D., Baranec, C., Baker, I., Jacobson, S., and Riddle, R., "Observatory deployment and characterization of SAPHIRA HgCdTe APD arrays," in [*High Energy, Optical, and Infrared Detectors for Astronomy VI*], *Proc. Soc. Photo-Opt. Instrum. Eng.* **9154**, 915419 (July 2014).

[6] Martinache, F., Guyon, O., Jovanovic, N., Clergeon, C., Singh, G., Kudo, T., Currie, T., Thalmann, C., McElwain, M., and Tamura, M., "On-Sky Speckle Nulling Demonstration at Small Angular Separation with SCExAO," *Pub. Astron. Soc. Pacific* **126**, 565–572 (June 2014).

[7] Mazin, B. A., Bumble, B., Meeker, S. R., O'Brien, K., McHugh, S., and Langman, E., "A superconducting focal plane array for ultraviolet, optical, and near-infrared astrophysics," *Opt. Express* **20**, 1503 (Jan. 2012).

[8] Close, L. M., Males, J. R., Morzinski, K., Kopon, D., Follette, K., Rodigas, T. J., Hinz, P., Wu, Y.-L., Puglisi, A., Esposito, S., Riccardi, A., Pinna, E., Xompero, M., Briguglio, R., Uomoto, A., and Hare, T., "Diffraction-limited Visible Light Images of Orion Trapezium Cluster with the Magellan Adaptive Secondary Adaptive Optics System (MagAO)," *Astrophys. J.* **774**, 94 (Sept. 2013).

[9] Lozi, J., Guyon, O., Jovanovic, N., Singh, G., Goebel, S., Norris, B., and Okita, H., "Characterizing and mitigating vibrations for SCExAO," in [*Adaptive Optics Systems V*], *Proc. Soc. Photo-Opt. Instrum. Eng.* **9909**, 99090J (July 2016).

[10] Petit, C., Sauvage, J.-F., Fusco, T., Sevin, A., Suarez, M., Costille, A., Vigan, A., Soenke, C., Perret, D., Rochat, S., Barrufolo, A., Salasnich, B., Beuzit, J.-L., Dohlen, K., Mouillet, D., Puget, P., Wildi, F., Kasper, M., Conan, J.-M., Kulcsár, C., and Raynaud, H.-F., "SPHERE eXtreme AO control scheme: final performance assessment and on sky validation of the first auto-tuned LQG based operational system," in [*Adaptive Optics Systems IV*], *Proc. Soc. Photo-Opt. Instrum. Eng.* **9148**, 91480O (Aug. 2014).

[11] Meimon, S., Petit, C., Fusco, T., and Kulcsar, C., "Tip-tilt disturbance model identification for Kalman-based control scheme: application to XAO and ELT systems," *J. Opt. Soc. Am. A* **27**, A122 (Sept. 2010).

[12] Petit, C., Conan, J.-M., Kulcsár, C., Raynaud, H.-F., and Fusco, T., "First laboratory validation of vibration filtering with LQG control law for Adaptive Optics," *Opt. Express* **16**, 87 (2008).

[13] Guyon, O. and Males, J., "Adaptive Optics Predictive Control with Empirical Orthogonal Functions (EOFs)," *Astron. J.* (July 2017).

[14] Singh, G., Lozi, J., Guyon, O., Baudoz, P., Jovanovic, N., Martinache, F., Kudo, T., Serabyn, E., and Kuhn, J., "On-Sky Demonstration of Low-Order Wavefront Sensing and Control with Focal Plane Phase Mask Coronagraphs," *Pub. Astron. Soc. Pacific* **127**, 857–869 (Oct. 2015).

[15] Singh, G., Lozi, J., Jovanovic, N., Guyon, O., Baudoz, P., Martinache, F., and Kudo, T., "A Demonstration of a Versatile Low-order Wavefront Sensor Tested on Multiple Coronographs," *Pub. Astron. Soc. Pacific* **129**, 095002 (Sept. 2017).